

PREDICTION OF STALL AND POST-STALL IN TWO- AND THREE-DIMENSIONAL FLOWS

Eric Besnard*, Bastien Puech†, Daniil Ivshin‡, Orhan Kural§, and Tuncer Cebeci**

Aerospace Engineering Department
California State University, Long Beach
1250 Bellflower Blvd.
Long Beach, CA 90840
Tel.: (562) 985-5442 - Fax: (562) 985-1669
besnarde@csulb.edu

Abstract

An efficient and accurate calculation method for the prediction of stall and post-stall of two- and three-dimensional high lift configurations is presented. The method is based on the interactive solution of the inviscid flow and boundary layer equations. The efficiency and robustness of the method have been improved by linearizing the turbulent terms in the boundary layer equations. Also, a model for surface roughness has been incorporated. The method is applied to the calculation of lift and drag coefficients about two- and three-dimensional configurations up to stall and post-stall conditions. Results show that the method predicts correctly the effects of Reynolds number and surface roughness on airfoil stall. For three-dimensional flows, the Reynolds number effects are also predicted. The paper shows the importance of an accurate calculation of wake flows for the prediction of the stall of three-element wings. In both two- and three-dimensional flows, the effects of Mach number are captured, provided the flow remains well below sonic conditions. In the contrary, a compressible inviscid flow method should be used in lieu of the panel method used here with compressibility corrections.

1. Introduction

Computational fluid dynamics (CFD) methods are now routinely used in the performance prediction and design of new aircraft, particularly at or near cruise conditions. One application where CFD still

lacks the required combination of accuracy and robustness is for the prediction of stall and post-stall of high lift configurations. The necessity of obtaining multiple solutions in a fast paced design environment further enhances the challenges facing the CFD community. In fact, even when the current growth rates in computer power are extrapolated, the direct numerical simulation (DNS) of three-dimensional high lift configurations is several decades away. Therefore, alternatives which meet both accuracy and efficiency requirements must be developed for use in aircraft high lift design.

For this purpose, the CFD community focuses mainly on the development of methods which solve the Reynolds-averaged Navier-Stokes (RANS) equations. While these methods, in particular the ones based on unstructured adaptive grids, promise to reach the desired objectives in some distant future, they still currently fall short of being efficient and accurate. Also, the transition calculation, critical for accurate drag¹ and Reynolds number effect² predictions, cannot be easily incorporated into the method. In particular, in light of the lack of significant progress in turbulence modeling over the past several decades, one may argue that the inaccuracy due to turbulence modeling will not justify the cost associated with using such methods for stall predictions if an affordable alternative providing reasonable accuracy exists.

The paper presents such an alternative which is based on interactive boundary layer (IBL) theory. Though not as general as the Navier-Stokes approach, it provides a good compromise between the efficiency and accuracy required in a design process.³ This approach involves the

* Lecturer, AIAA Member

† Visiting Research Student, Ecole Polytechnique, France

‡ Undergraduate Student, AIAA Student Member

§ Professor

** Professor and Chair, AIAA Fellow

interactive solution of the inviscid, boundary-layer, and stability equations. For low speed flows, the inviscid flow is often computed by a panel method (with or without compressibility corrections) or by a full-potential flow method, and the viscous flow is computed by a boundary-layer method. The transition calculation is easily incorporated into the method. The method was previously presented and applied to the prediction of lift and drag coefficients of single and multi-element wings at high lift.⁴ The present paper addresses issues pertaining to the prediction of stall and focuses in particular on the study of Reynolds number, surface roughness, and compressibility effects on stall.

The calculation method is briefly described in Sect. 2, focusing on recent improvements and additions. Sample results for two- and three-dimensional high lift flows are shown in Sects. 3 and 4, respectively. In both cases, Reynolds number and compressibility effects are investigated. The paper ends with a summary of the more important conclusions.

2. Calculation method

The calculation method is similar for both two- and three-dimensional flows. The method for two-dimensional flows has been used extensively for predicting the flow about single and multi-element airfoils.¹ Its three-dimensional counterpart is presented in Ref. 4 where it is applied to the prediction of lift and drag coefficients of single and multi-element wings. Only a brief description is included here, focusing on recent improvements incorporated for the purpose of stall and post-stall predictions.

2.1. Summary of the method

The ingredients of the method are shown in Fig. 1.

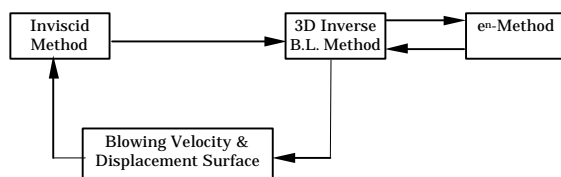


Fig. 1. Interactive Boundary Layer method

In the present study, the inviscid flow is computed by the higher-order Hess panel method,⁵ which is applicable to a complete airplane configuration. Alternatively and without loss of generality, an Euler or full potential method could be substituted to the panel method.

Once the velocity components have been determined with the inviscid method, they are transformed into a non-orthogonal body-fitted coordinate system generated on the wing surface. The boundary layer equations for the non-orthogonal coordinate system are solved in inverse mode to allow for the computation of separated flow.⁶

If necessary, at this point, the laminar velocity and temperature profiles are used to solve the three-dimensional compressible linear stability equations using the Saddle Point method of Cebeci and Stewartson to determine the transition location.⁶

Then, the boundary layer calculations are continued from the calculated transition location up to the trailing edge and into the far wake. Turbulent flow calculations are performed using a modified Cebeci-Smith eddy-viscosity formulation⁷ extended to three-dimensional flows.

Once the boundary layer equations have been solved, the displacement surface and blowing velocity distributions on the wing and in the wake are computed. The blowing velocity is used as boundary condition on the panels and the Kutta condition is satisfied at the displacement surface. The procedure is repeated until convergence is reached.

2.2. New features

Three main features have been recently added to the method. The first one deals with the extension of improvements in the turbulence model to three-dimensional flows. The second one deals with the addition of an existing model to treat rough surfaces, and the last one corresponds to improvements in convergence and robustness through turbulence term linearization.

Turbulence model for three-dimensional separated flows

The method employs a modified Cebeci-Smith turbulence model⁷ which has been recently extended and validated for three-dimensional flows in a strong adverse pressure gradient leading to flow separation⁴ and which gave results in close agreement with experimental data and Reynolds stress models. Also, another test case showed that the stall of a single wing could be accurately predicted with the modified model, when it could not with the original one.⁴

Turbulence model for rough surfaces

The flow properties, in particular near stall conditions, greatly depend on surface conditions. These also play a key role in accurate drag

predictions at lower angles of attack, and therefore, must be modeled in the calculation method.

For given roughness height (k) and roughness density (λ), an equivalent sand grain roughness parameter, k_s , can be determined.^{8,9} For rough surfaces, the length scale in the eddy viscosity formulation⁴ can be modified as a function of the equivalent sand grain roughness parameter, such that

$$\ell = 0.4(y + \Delta y)(1 - \exp(-(y + \Delta y)/A))$$

where Δy in terms of dimensionless quantities k_s^+ and Δy^+ is given by¹⁰

$$\Delta y^+ = \begin{cases} 0 & k_s^+ < 5 \\ 0.9 \left(\sqrt{k_s^+} - k_s^+ \exp(-k_s^+/6) \right) & 5 \leq k_s^+ < 70 \\ 0.7(k_s^+)^{0.58} & 70 \leq k_s^+ \leq 2000 \end{cases}$$

where k^+ is the roughness Reynolds number given by

$$k^+ = \frac{u_\theta k}{\nu}$$

and other variables are the classical ones used in boundary layer theory.

Turbulence term linearization

One of the key improvements in speed and robustness stems from the introduction of partial linearization of the turbulence terms in the solution of the boundary layer equations.

At any given location on the wing or in the wake, the solution of the boundary layer equations requires several steps:

- Transform the equations, their boundary conditions, and the Hilbert integral equation using a variation of the Falkner-Skan transformation suitable for inverse mode (the velocity at the edge of the boundary layer is unknown),
- Simplify the equations using the quasi three-dimensional approximation,
- Transform the equations into a system of first order partial differential equations,
- Discretize the equations using central differences in the direction normal to the wall and 2-pt backward differences in the streamwise direction for second order accuracy,
- Linearize the system with Newton's method,
- Invert the system, and solve for the next iteration until convergence is reached.

While for laminar flows it is customary to fully linearize the boundary layer equations

with Newton's method so that the convergence rate is quadratic, it is not customary to linearize the turbulence terms, thus reducing the convergence rate and possibly leading to oscillations which may prevent convergence. A partial linearization of the turbulence terms was introduced¹¹ leading to a significant increase in convergence rates, particularly in the case of separated flow, and to a higher robustness of the method, both of which are essential characteristics for the calculation of stall and post-stall conditions.

A sample of results is presented here for a wing with 30° sweep with an Eppler 387 airfoil cross-section at $Re = 200,000$ and $\alpha = 4^\circ$ so that a large separation bubble (about a quarter chord) is present on the wing upper surface. Two x -locations at $\eta_b = 0.26$ are selected, $x/c = 0.65$ and 0.98 , identified by $NX = 50$ and 75 , respectively. For $NX = 50$, the flow is turbulent and separated and for $NX = 65$, the flow is turbulent and attached. Fig. 2 shows the maximum residual across the boundary layer with quasi-Newton iterations. Here V denotes the derivative of U with respect to the coordinate normal to the wall in the computational domain. Drastic improvements in convergence rates are observed, in particular for the case of separated flow.

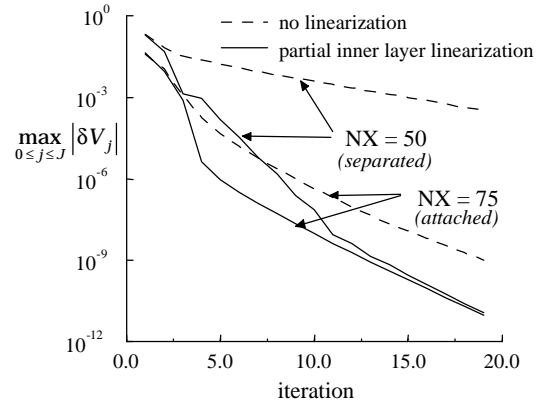


Fig. 2. Partial linearization of turbulent terms and convergence acceleration.

3. Stall predictions for two-dimensional high lift flows

A sample of results is presented here to illustrate the capabilities of the method for predicting airfoil stall. For incompressible flows, the effects of Reynolds number and roughness on stall are investigated and compared with experimental data in Sect. 3.1. Results for compressible flows are presented in Sect. 3.2. Finally, sample results for multi-element airfoils are shown in Sect. 3.3.

3.1. Single element airfoils in incompressible flows

Effect of Reynolds number

Fig. 3 presents a comparison between measured^{12,13} and calculated maximum lift coefficients, $c_{l,max}$, for a variety of single element airfoils as a function of Reynolds number. Results show good agreement between calculations and experimental data, except for the FX 74-CL5-140 and FX 72-MS-150B airfoils at $Re = 10^6$ where transition location may have been at the source of the discrepancy.

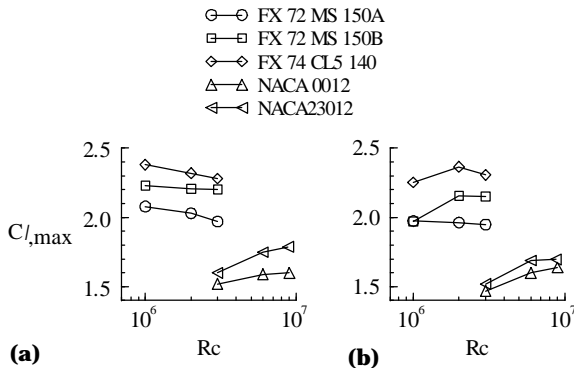


Fig. 3. $C_{l,max}$ for several airfoils at various Reynolds numbers, (a) measured and (b) calculated.

In all cases above, the flow velocity was sufficiently low ($M_\infty < 0.15$), so that incompressible flow could be assumed. Results show that, overall, the method is able to predict the effect of Reynolds number on maximum lift coefficient for single airfoils.

Effect of roughness

Fig. 4 shows the effect of leading edge roughness on the aerodynamic performance of the NACA 0012 airfoil when roughness elements of $k/c = 0.00025$ are distributed on the first 8% chord of the upper and lower surfaces. Results agree well with experimental data up to stall and post-stall conditions for both lift and drag coefficients. Several other airfoils (e.g. NACA 4412, NACA 23012, etc.) were tested and a similar agreement between data and calculations was observed.

3.2. Single element airfoils in compressible flows

The case of single airfoils in compressible flows ($M_\infty > 0.2$) is addressed here by considering the flow about a NASA supercritical airfoil tested at several Mach numbers.

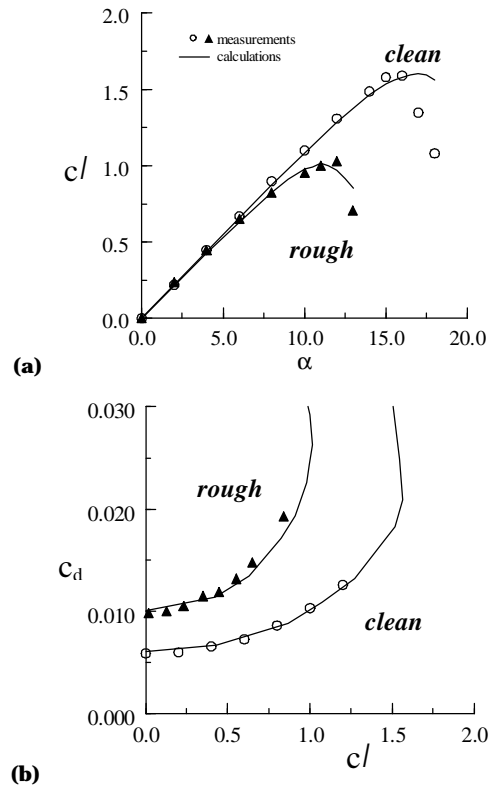


Fig. 4. Effect of roughness on NACA 0012 airfoil aerodynamic performance at $Re = 6 \times 10^6$, (a) lift and (b) drag coefficients.

Fig. 5 shows a comparison between measurements,¹⁴ compressible Navier-Stokes calculations using the same version of the CS turbulence model,⁷ and results obtained with the present IBL method for two free stream Mach numbers, $M_\infty = 0.201$ and 0.284 . The corresponding chord Reynolds numbers are $Re = 4.02 \times 10^6$ and 2.83×10^6 .

Unfortunately, the Reynolds number is not constant, making it difficult to determine the exact source of the discrepancies between data and predictions. It is interesting to note, however, that at $M_\infty = 0.201$ stall is slightly under-predicted with the IBL method and correctly predicted with the compressible Navier-Stokes method when the opposite holds for $M_\infty = 0.284$. The reduction in $C_{l,max}$ due to the increase in Mach number is less drastic with the IBL method than with the Navier-Stokes method or the one measured in wind tunnel. These results suggest that, even though stall predictions are satisfactory with the IBL method, some effects due to compressibility may not be correctly taken into account. In fact, this comes to no surprise since critical (sonic) flow occurs near stall and, therefore, the compressibility corrections in the panel method are no longer valid.

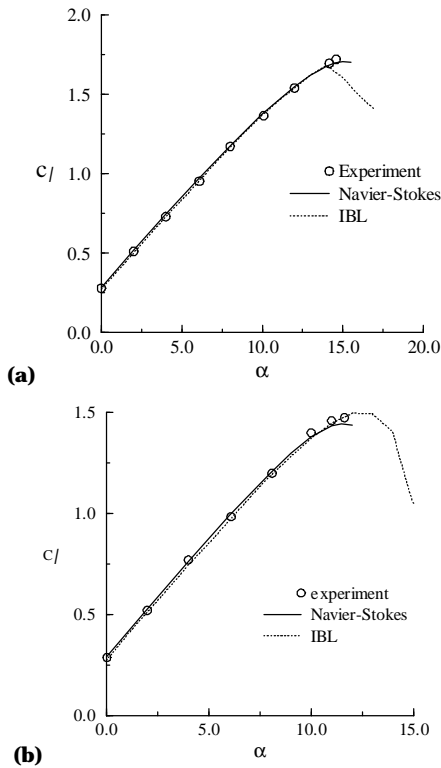


Fig. 5. Lift coefficient for a NASA supercritical airfoil, (a) $M = 0.201$ and $Rc = 2.83 \times 10^6$, and (b) $M = 0.284$ and $Rc = 4.02 \times 10^6$.

Despite this remark and considering the efficiency of the method when compared with its compressible Navier-Stokes counterpart, the stall predictions with the IBL method can be considered satisfactory. Also, this problem could be alleviated by using a full-potential flow solver in lieu of the panel method used here.

3.3. Multi-element airfoils

The calculation method has been extensively used for the prediction of flows about multi-element airfoils^{1,6,15} and only a sample of results is presented here.

Wind tunnel measurements were performed on several three-element airfoil configurations at the NASA Langley Low Turbulence Pressure Tunnel (LTPT) at various Reynolds and Mach numbers.¹⁶⁻¹⁸ The test case considered here has the slat and the flap deflected at 30° with gap/overlap riggings of $0.0295c/-0.025c$ and $0.0127c/0.0025c$, respectively, where c is the airfoil chord with slat and flap retracted. The configuration is shown in Fig. 6. The test Reynolds number was 9×10^6 and the free stream Mach number was 0.2. Lift, drag and moment coefficients are presented in Fig. 7 and compared with experimental data. Several experimental data sets were available¹⁹ and are

represented. It is important to note that the present results were obtained without using the experimental transition location, because, in general, the designer does not have that information. Instead, the transition predicted by the calculation method was used.



Fig. 6. Three-element airfoil configuration

The lift coefficients are slightly over-predicted, possibly due to modeling approximations used in the IBL method, such as in coves, and/or due to experimental setup, such as wall effects. Fig. 8 shows a comparison between measured and calculated pressures near stall conditions and shows that agreement is also quite satisfactory. Also, the calculation method was applied to the prediction of changes in force coefficients when the flap positioning is modified and when the Reynolds number is reduced to 5×10^6 . Results showed a satisfactory comparison between measurements and calculations, including near or at stall conditions.¹⁵

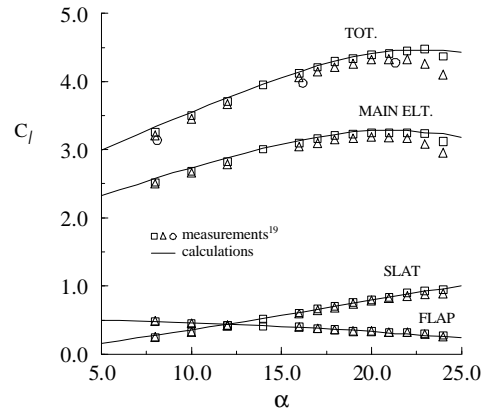


Fig. 7. Comparison of measured and calculated lift coefficients for the three-element airfoil

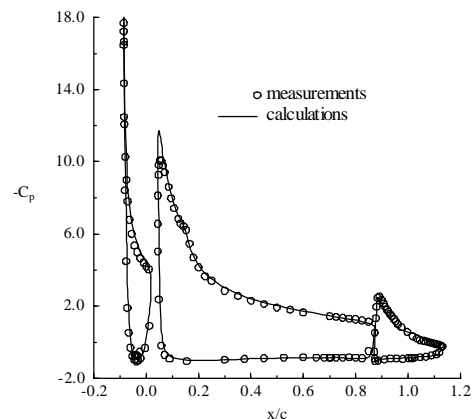


Fig. 8. Measured and calculated pressure coefficient for the baseline configuration at $\alpha = 21.34^\circ$

4. Stall predictions for three-dimensional high lift flows

4.1. Wing-body configuration

In a previous paper,⁴ the method was applied to the prediction of lift and drag coefficients of a wing with various high lift systems. The method was able to predict the stall of the wing with slat and flap retracted. The present paper extends the study reported therein by investigating the effects of Reynolds and free stream Mach numbers on stall predictions. However, unlike for two-dimensional flows, where a large set of experimental data is available, very little measurements have been reported in the literature for three-dimensional flows near stall. Therefore, no experimental data measuring these effects was available.

In order to be able to qualitatively analyze the predictions of the current method, results at various Reynolds and Mach numbers are compared with those obtained using a validated semi-empirical method, the “pressure difference

20

The wing-body configuration considered here was tested in wind tunnel at transonic conditions at what was Douglas Aircraft Company²¹ and is known as the LB-488 wing-body. It is used here for low speed tests because it is representative of a typical transport aircraft (twisted tapered wing with several kinks). A paneling of the wing-body configuration is shown in Fig. 9.

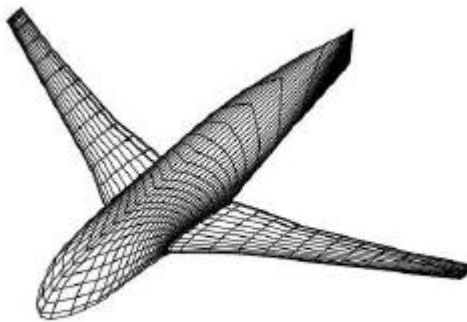
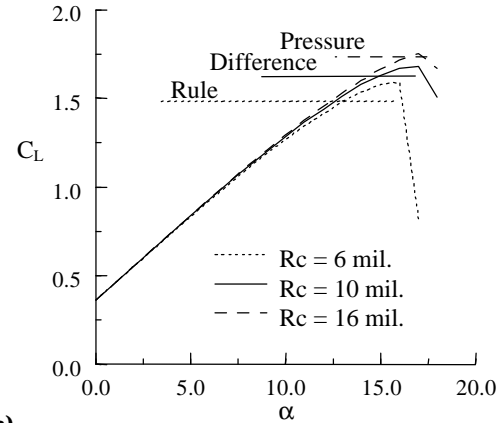


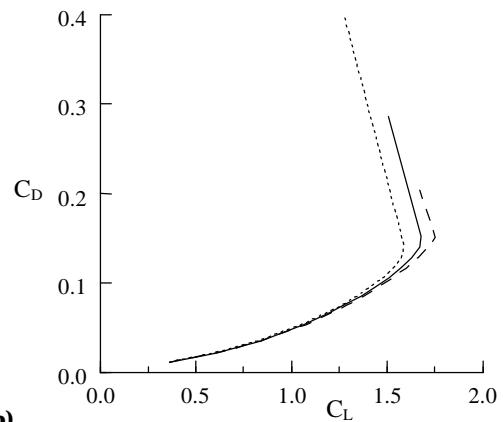
Fig. 9. Partial paneling of the wing-body configuration

Fig. 10 shows the calculated lift and drag coefficients at $M_\infty = 0.2$ and $R_C = 6 \times 10^6$, 10×10^6 and 16×10^6 . Also shown are the corresponding maximum lift coefficients calculated using the PDR. It is seen that the IBL method over-estimates the maximum lift

coefficient at the lower Reynolds numbers with respect to the PDR and that the discrepancy between the two methods diminishes as the Reynolds number is increased. Not surprisingly, both methods predict an increase in maximum lift coefficient with an increase in Reynolds number.



(a)



(b)

Fig. 10. Force coefficient variation with Reynolds number at $M_\infty = 0.2$ for the LB-488 wing-body, (a) lift and (b) drag

Fig. 11 shows a similar comparison at a fixed Reynolds number of $R_C = 6 \times 10^6$ when the Mach number varies from 0.15 to 0.25. In this case, however, the PDR predicts a decrease in maximum lift coefficient – which is to be expected – while the maximum lift coefficient is barely affected in IBL method predictions. Agreement between the two methods is excellent for $M_\infty = 0.15$ ($C_{L,MAX} = 1.58$ with the IBL method and 1.59 with the PDR) and deteriorates already at $M_\infty = 0.2$ (1.59 vs. 1.48), suggesting that the IBL method does not correctly predict the compressibility effects even at this fairly low free stream Mach number. The calculated local Mach number along the wing chord is shown in Fig. 12 at the critical spanwise station (section where the local Mach number is maximum) at the stall angle. Since for $M_\infty = 0.2$ the local Mach number peaks at about

0.8 for a very short distance, it is hard to conclude whether the discrepancy comes from an inaccurate inviscid calculation or inaccuracies in the PDR. The latter would not be surprising since the PDR is based on two-dimensional data while the present wing is significantly swept. For $M_\infty = 0.25$, the difference between the PDR and IBL methods further increases. In this case, however, in light of the results shown in Fig. 12, one should not expect to obtain reliable results with the IBL method near stall.

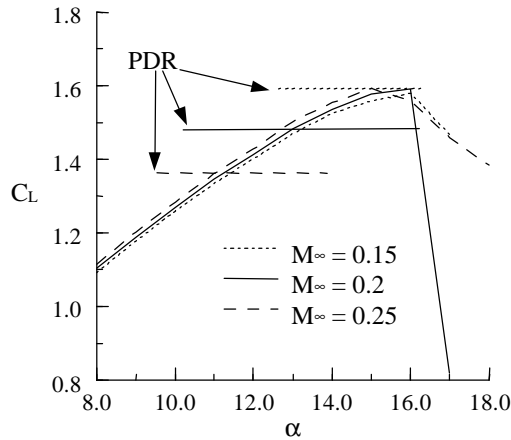


Fig. 11. Lift coefficient at $Re = 6 \times 10^6$ for the LB-488 wing-body

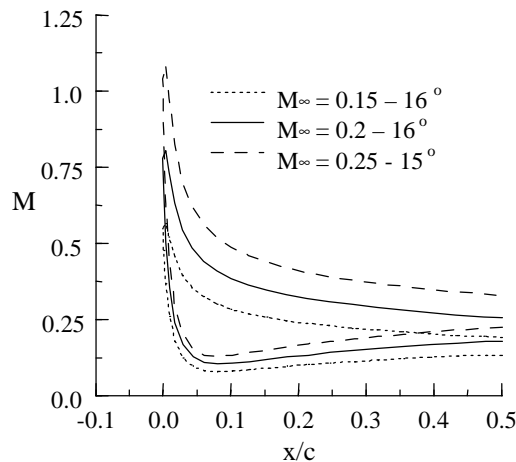


Fig. 12. Calculated local Mach number distribution at the critical spanwise location at $Re = 6 \times 10^6$

These results clearly demonstrate that, even for low free stream Mach numbers (in particular around 0.25 or higher), a truly compressible flow solver should be used for accurate stall predictions and that the grid should be refined near the leading edge to capture non-linear effects or possible weak shocks. Work is in progress to further investigate these compressibility effects on wing stall and to

determine “how far” a panel method could be used for such configurations without loss of accuracy. In particular, results will be compared with those obtained with a compressible flow solver.²² The case of inviscid flow is being investigated first to avoid any differences arising due to turbulence modeling.

4.2. Wing with slat and flap deployed

In Ref. 4, the method was also applied to the prediction of both lift and drag coefficients of a wing with high lift systems deployed. Results showed good agreement between calculations and experimental data reported by Lovell²³ for a wing which has an aspect ratio of 8.35, a quarter chord sweep angle of 28° , and a taper ratio of 0.35. Fig. 13 shows the paneling distribution of the wing with both slat and flap deflected at 25° . In this case, however, stall was not captured by the prediction method.⁴

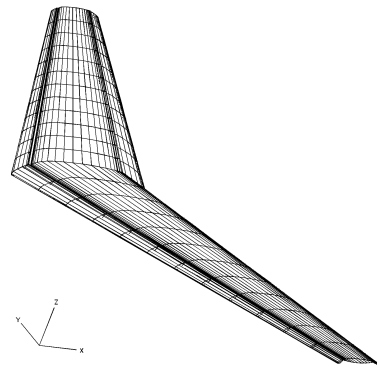


Fig. 13. Multi-element wing paneling with slat and flap deployed at 25° - wakes omitted.

Previous results for two-dimensional flows showed the importance of accurate calculations in the wake regions, in particular when a slat is deployed.¹ With the present three-dimensional panel method, however, the wake location – used in the inviscid method to shed vorticity and in the boundary layer method to model the viscous effects in the wake region – is fixed. To investigate the importance of the wake location, calculations were repeated with several wake shapes.

The wake shapes are generated at a fixed angle of attack using a two-dimensional panel method (with viscous effects), and the same shape is scaled and used all along the wing span (the present wing cross-section does not change). Fig. 14 shows the calculated wake shapes for $\alpha_{2D} = 5, 13, \text{ and } 21^\circ$ which correspond to two-dimensional lift coefficients of 2.5, 3.5, and 4.2, respectively. Fig. 15 shows a comparison between the pressure distribution at the critical spanwise station

($\eta \approx 0.8$) at $\alpha_{3D} = 19^\circ$ and those calculated for two-dimensional flows. This pressure distribution shows that the local airflow incidence at this spanwise station is close to 13° . The three-dimensional pressure coefficient on the flap, however, agrees better with the results of $\alpha_{2D} = 21^\circ$, which suggests that the wakes above the flap are probably farther away from the flap in the normal direction than calculated at 13° . Here, the three-dimensional results correspond to those obtained with the wake shape at 13° . The differences between the results obtained for three-dimensional flows with the three wake shapes were small compared with the differences between the various angles of attack for two-dimensional flows.

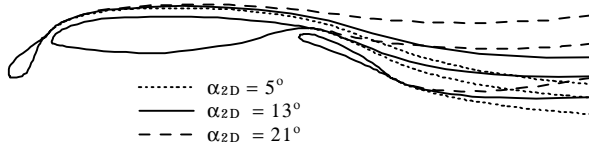


Fig. 14. Calculated wake shapes in two-dimensional flows

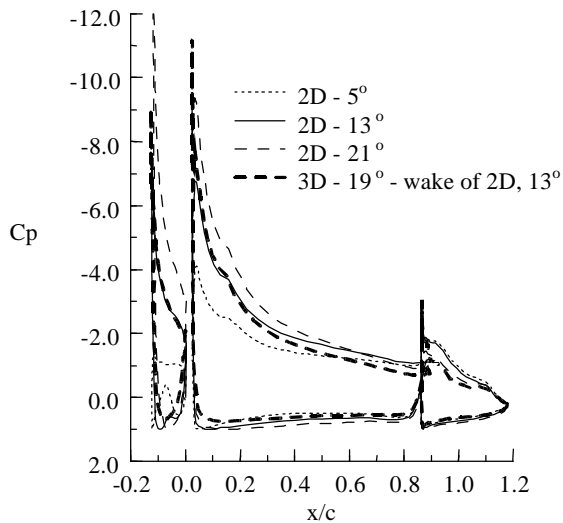
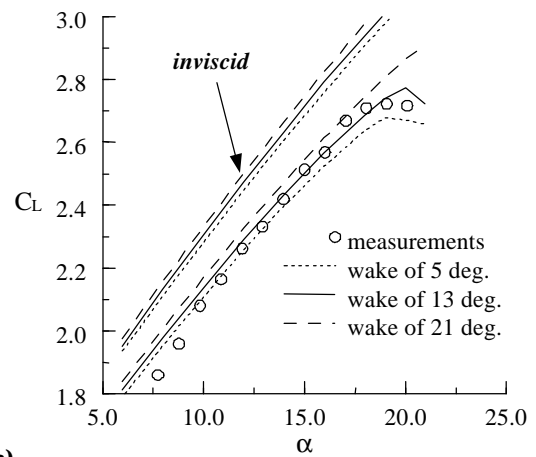
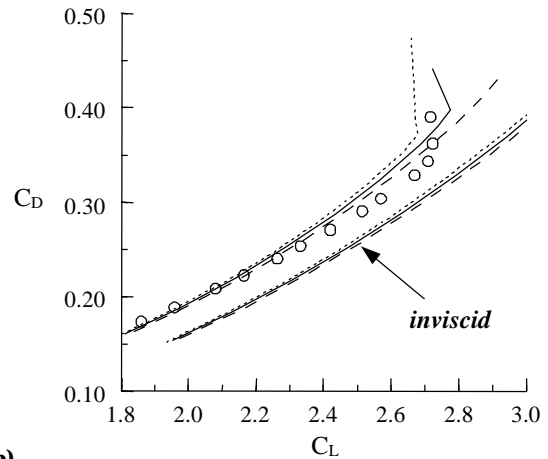


Fig. 15. Comparison between pressure distribution at $\alpha_{2D} = 5, 13,$ and 21° and $\alpha_{3D} = 19^\circ$ ($\eta \approx 0.8$)

Therefore, one should expect better predictions near stall ($\alpha_{3D} = 19^\circ$) when the wake shape of $\alpha_{2D} = 13^\circ$ is used than for the others. Fig. 16, which shows a comparison between measured and calculated lift and drag coefficients using all three wake shapes, supports this intuitive reasoning, even if the lift coefficient at stall is slightly over-predicted.



(a)



(b)

Fig. 16. Wing with slat and flap deployed at 25° : (a) lift and (b) drag coefficients.

Figs. 17 and 18 further demonstrate the importance of capturing the flow behavior in the main element wake for three-element airfoils and wings. When a slat is deployed, the pressure gradient on the main element upper surface is greatly reduced and stall may not be initiated by flow separation on the body of the main element. Instead, the boundary layer at the main element trailing edge is thick, but attached, and still has to negotiate the pressure gradient created by the deployed flap. In this case, stall may be initiated by off-body re-circulation above the flap. This phenomenon is clearly observed in Fig. 17 for the wake shape of $\alpha_{2D} = 13^\circ$ which depicts the minimum velocity variation in the wake at the critical spanwise station. The corresponding drastic increase in wake displacement thickness is shown in Fig. 18.

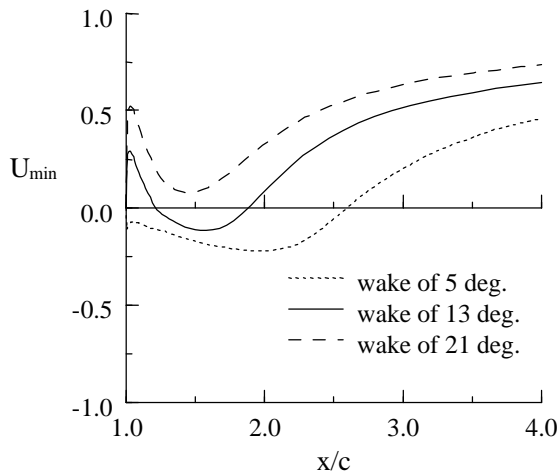


Fig. 17. Minimum velocity distribution in the main element wake at the critical spanwise station for $\alpha = 20^\circ$.

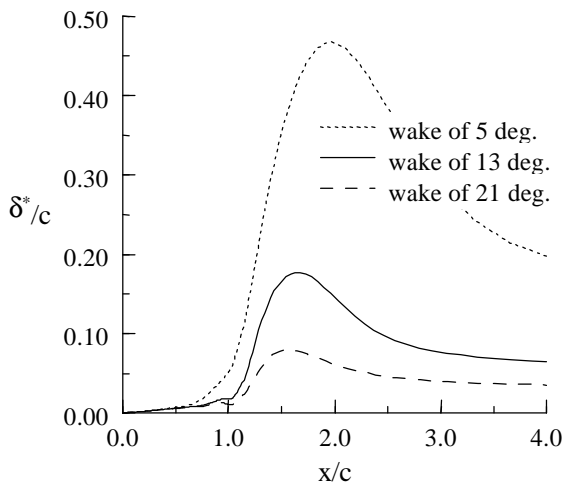


Fig. 18. Displacement thickness distribution on the main element body and wake at the critical spanwise station for $\alpha = 20^\circ$.

Overall, these results show that an accurate calculation of the wake flow is important for precise stall predictions. They also show that the present method could be used successfully to predict the stall of multi-element wing configurations, provided an iterative wake shape calculation procedure was incorporated in the method.

5. Concluding remarks

A method based on an interactive-boundary-layer approach for predicting the single and multi-element airfoils and wings is described. Recent improvements to the method include the addition of a model for rough surfaces, improvements to the turbulence model, and the introduction of partial linearization of the turbulence terms to increase convergence rates

and robustness, in particular for separated flows. The calculation method is applied to the prediction of airfoil and wing stall at high lift. Results show that the method predicts correctly the effects of Reynolds number and surface roughness on airfoil stall. For three-dimensional flows, the Reynolds number effects are also predicted. The paper shows the importance of an accurate calculation of wake flows for the prediction of the stall of three-element wings. In both two- and three-dimensional flows, the effects of Mach number are captured, provided the flow remains well below sonic conditions. If the flow reaches speeds close to supersonic, a compressible inviscid flow method should be used in lieu of the panel method used here with compressibility corrections.

The paper emphasizes the need for developing a comprehensive experimental database for three-dimensional low speed separated flows at high lift. For the few test cases available, the method is shown to be reliable provided the conditions described above (wake shape and truly compressible flow solver) are met. Work is currently in progress to incorporate these features so that the method may become an even more useful tool for routine three-dimensional high lift system design.

References

1. T. Cebeci, E. Besnard and H.H. Chen, "An Interactive Boundary-Layer Method for Multielement Airfoils," *Computers & Fluids*, Vol. 27, No. 5-6, pp. 651-661, 1998.
2. Arlinger B.G. et al., "Reynolds- and Mach-number Effects and 2D-3D Correlation Based on Measurements and Computed Results for the Garter Take-off Configuration," *Proceedings of High Lift and Separation Control*, Royal Aeronautical Society, London, March 1995.
3. N.B. Nield, "An Overview of the 777 High Lift Aerodynamic Design," *Proceedings of High Lift and Separation Control Conference*, Royal Aeronautical Society, March 1995.
4. E. Besnard, O. Kural, and T. Cebeci, "Flow Predictions about Three-dimensional High Lift Systems," AIAA Paper No. 99-0543, Jan. 1999.
5. J.L. Hess, "Calculation of Potential Flows About Arbitrary Three-dimensional Lifting Bodies," MDC Report No. J5679-01, 1972.
6. T. Cebeci, *An Engineering Approach to the Calculation of Aerodynamic Flows*, Horizon Publishing Inc., Long Beach, CA, 1999.

7. T. Cebeci and K.C. Chang, "An improved Cebeci-Smith turbulence model for boundary-layer and Navier-Stokes methods," *Proceedings of the 20th ICAS/AIAA Aircraft System Conference*, Italy, 1996.
8. H. Schlichting, *Boundary Layer Theory*, McGraw-Hill, New York, 1968.
9. F. A. Dvorak, "Calculation of Turbulent Boundary Layers on Rough Surfaces in Pressure Gradient," *AIAA Journal*, Vol. 7, Sept. 1969, pp. 1752-1759.
10. T. Cebeci and K.C. Chang, "Calculation of Incompressible Rough-Wall Boundary-Layer Flows," *AIAA Journal*, Vol. 16, July 1978, pp. 730-735.
11. E. Besnard, "Prediction of High Lift Flows with Separation," Ph.D. dissertation, Claremont Graduate University and California State University, Long Beach, May 1998.
12. M.S. Selig and J.J. Guglielmo, "High-Lift Low Reynolds Number Airfoil Design," *J. Aircraft*, Vol. 34, No. 1, Jan. 1997.
13. I.H. Abbott and A.E. Von Doenhoff, *Theory of Wing Sections*, Dover, 1959.
14. E. Omar, T. Zierten and A. Mahal, "Two-Dimensional Wind Tunnel Tests of a NASA Supercritical Airfoil with Various High Lift Systems," NASA CR-2215, 1977.
15. E. Besnard, A. Schmitz, E. Boscher, N. Garcia, and T. Cebeci, "Two-dimensional Aircraft High Lift System Design and Optimization," AIAA Paper No. 98-0123, Jan. 98.
16. W.O. Valarezo, "High Lift Testing at High Reynolds Numbers," AIAA Paper 92-3986, July 1992.
17. V.D. Chin, D.W. Peter, F.W. Spaid, and R.J. McGhee, "Flowfield Measurements About a Multi-element Airfoil at High Reynolds Numbers," AIAA Paper 93-3137, July 1993.
18. F.W. Spaid and F.T. Lynch, "High Reynolds Number, Multi-element Airfoil Flowfield Measurements," AIAA Paper 96-0682, Jan. 1996
19. F.T. Lynch, R.C. Potter, and F.W. Spaid, "Requirements for Effective High Lift CFD," *Proceedings of the 20th ICAS/AIAA Aircraft System Conference*, Sept. 1996.
20. W.O. Valarezo and V.D. Chin, "Maximum Lift Prediction for Multielement Wings," AIAA Paper No. 92-0401, Jan. 1992.
21. L.T. Chen and M.N. Bui, "An Interactive Scheme for Transonic Wing/Body Flows Based on Euler and Inverse Boundary-Layer Equations," AIAA Paper No. 90-1586, June 1990.
22. P.G. Buning *et al.*, "Overflow User's Manual," V. 1.81, NASA Ames, July 1999.
23. D. A. Lovell, "A wind-tunnel investigation of the effects of flap span and deflection angle, wing planform and a body on the high-lift performance of a 28° swept wing," R.A.E., C.P. No. 1372, Farnborough, U.K, 1977.